

Formation of Convective Cells, Anomalous Diffusion, and Strong Plasma Turbulence Due to Drift Instabilities*

C. Z. Cheng and H. Okuda

Plasma Physics Laboratory, Princeton University, Princeton, New Jersey 08540

(Received 26 January 1977)

Large-scale, fully three-dimensional particle simulations have been carried out for the collisionless drift instabilities in a cylindrical geometry. It is found that nonlinear excitation of convective cells ($\omega = 0, k_{\parallel} = 0$) due to drift instabilities gives rise to enhanced turbulence and anomalous plasma diffusion. The observed power spectra have resemblance with the recent measurements in toroidal devices.

Here we report our recent results of numerical simulations on collisionless drift instabilities using large-scale fully three-dimensional cylindrical plasma models developed earlier.¹ Theoretical interpretations of the observed results on plasma turbulence and diffusion are also given. Drift-wave turbulence has been of current interest in toroidal confinement devices such as tokamaks,² stellarators,³ and internal ring devices^{4,5} because of the strong correlation between the observed density fluctuations and anomalous plasma transport.

The simulation model used is a straight cylinder in a uniform external magnetic field B_0 along the z direction with its length $L_z/\rho_i = 640$, $\rho_i = (T_i/m_i)^{1/2}/\Omega_i$ being the ion gyroradius. In the cross section, a 64×64 (L^2) spatial grid is used for numerical computation with its physical length $L/\rho_i = 32$. The plasma is periodic in z while it is surrounded by a conducting wall at the boundary of the cross section.¹ Initially both ions and electrons have Maxwellian velocity distributions with $T_e/T_i = 4$. Initial plasma density is taken to be $n_e(r) = n_i(r) = n_0 \exp(-4r^2/a^2)$ with the average density given by $\Omega_e/\omega_{pe} = 5$, $m_i/m_e = 100$, $a = L/2$; and there is no initial temperature gradient. Seven Fourier modes $n = 0, \pm 1, \pm 2$, and ± 3 are kept in the z direction with $k_z = 2\pi n/L_z$. Linear theory predicts that the collisionless drift instability (universal mode) is strongly unstable for $n = \pm 1$ and becomes stable rapidly with increasing $|n|$ because of the onset of ion Landau damping. This situation is commonly observed in Q devices. In terms of physical size, the simulation plasma is certainly smaller than a tokamak plasma but may be larger than a conventional Q device; and one can study quite a few problems with the model using realistic plasma parameters.

Let us first look at the gross behavior of the instability. Figure 1 shows the particle diffusion, heat transfer, electron velocity distribution, and radial-mode structure associated with the insta-

bility. While ions and electrons diffuse more or less together in the early stage, we see large charge separation built up at a later stage because of the difference of radial cE_{θ}/B drifts of ions and electrons, where E_{θ} is the azimuthal electric field associated with the drift wave. As will be shown later, this charge separation generates strong two-dimensional electric fields which, in turn, excite large amplitude convective cells ($\omega = 0, k_{\parallel} = 0$). The observed anomalous particle diffusion is mainly due to drift instabilities at the early stage; and at the later stage, it is due to nonlinearly excited convective cells, which enhance diffusion even when the drift instability is quenched.

The electron parallel temperature $T_{e\parallel}$ rapidly decreases for $r/a > 0.5$ because of inverse Landau

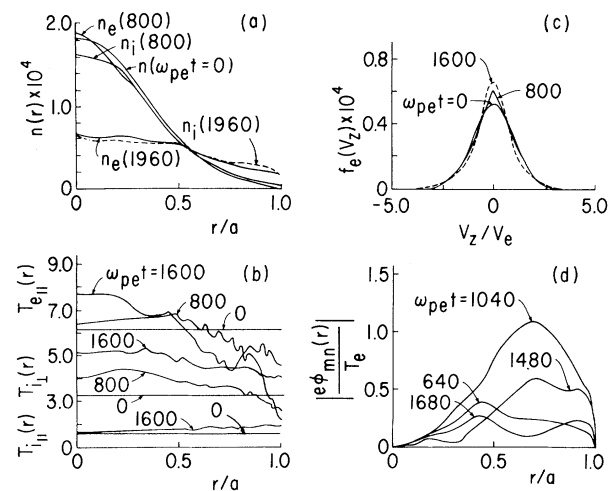


FIG. 1. Time variation of (a) ion and electron density profiles $n_i(r)$ and $n_e(r)$ in terms of number of particles summed over a given volume; (b) electron parallel temperature $T_{e\parallel}(r)$, ion parallel temperature $T_{i\parallel}(r)$, and ion perpendicular temperature $T_{i\perp}(r)$ in terms of thermal electron energy $m_e v_e^2/2 = 6.2$; (c) electron velocity distribution; and (d) radial-mode structures for the $(m, n) = (3, 1)$ mode.

damping and increases for $r/a < 0.5$ because of the absorption of wave energy associated with the radial convection. The electron parallel-velocity distribution steepens because of inverse Landau damping.⁶ Ion perpendicular temperature $T_{i\perp}$ increases through the acceleration across the magnetic field associated with the short-wavelength turbulence due to the convective cells. Ion parallel temperature $T_{i\parallel}$ changes little because ion Landau damping is weak. A typical drift-wave radial-mode structure $(n=1, m=3) |e\varphi(r)/T_e|$ shows a peak near $r/a=0.5$ at the early stage, consistent with the initial density profile. After reaching the maximum amplitude of 10% at $\omega_{pe}t = 1040$, it begins to level off as a result of nonlinear excitation of convective cells ($n=0$).

Figure 2 shows more detailed diagnostics of the instability: spectral distributions $|E^2(m)|$ and $|E^2(n)|$, and power spectrum $P_{mn}(\omega, r)$ with respect to k_θ and k_z , where m is the azimuthal mode number with $k_\theta = m/r$. $|E^2(m)|$ indicates typical spectral profile for drift turbulence as seen in the experiments²; it peaks around $k_\theta \rho_i = 0.3 \sim 0.6$, corresponding to the $m=2, 3$, and 4 modes for this case. The amplitude decreases rapidly for $k_\theta \rho_i \gtrsim 1$ ($m \gtrsim 8$). The shape of the spectral distribution does not change much in the nonlinear stage except for the shift of the peak of

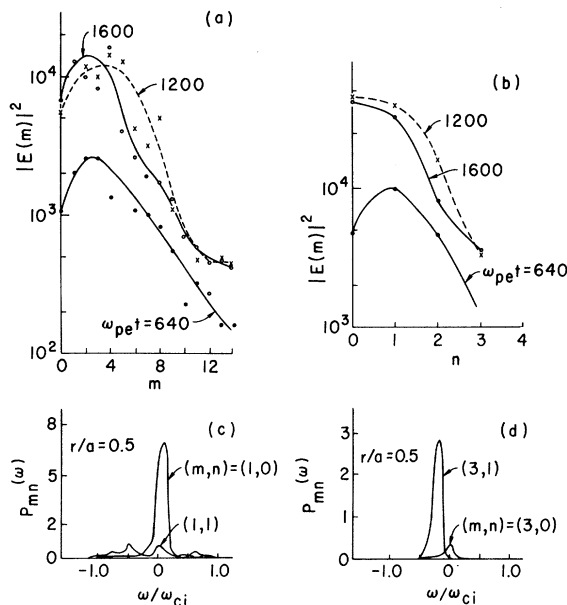


FIG. 2. Time variation of (a) spectral distribution $|E^2(m)|$ and (b) spectral distribution $|E^2(n)|$. Power spectra for (c) the $(m,n)=(1,1)$ and $(1,0)$ modes and for (d) the $(m,n)=(3,1)$ and $(3,0)$ modes indicate two peaks near $\omega \approx 0$ and ω^* .

the spectrum toward low m numbers. This is due to the nonlinear excitation of convective cells which tend to coalesce into larger cells. $|E^2(n)|$, on the other hand, indicates a drastic change when the instability develops into a nonlinear regime. We see that at earlier times the spectrum is peaked at $n=1$ ($k_z = 2\pi/L_z$) and decreases rapidly with increasing n . This is quite reasonable because the growth rate for $n=2$ and 3 are much smaller. The $n=0$ mode, which may be called convective-cell modes ($k_z=0, \omega=0$), also grows as the drift instability grows; and eventually they dominate over the drift instability. Note that this is not the ambipolar field ($m=n=0$). The excitation of convective cells is clearly seen in the power-spectrum plots $P_{mn}(\omega)$ at $r/a=0.5$, where we see both drift modes ($n \neq 0, \omega \neq 0$) and convective cells ($n=0, \omega=0$). For the $m=3$ modes, the power spectrum indicates that the amplitude of drift mode ($n=1$) is much larger than the convective cells ($n=0$), while for $m=1$, convective cells are much stronger than the drift mode.

The physical mechanism of the excitation of convective cells is the following. Consider a drift-wave fluctuation $\varphi(r, \theta, z, t) = \varphi_{mn}(r) \exp[i(\omega t - m\theta - k_z z)]$. Both ions and electrons will move through the cE_θ/B_0 drift in the radial direction. For a linearly unstable drift wave, $v_i \ll \omega/k_z \ll v_e$ is satisfied so that the electron cE/B_0 drift tends to be averaged out on the time scale of drift wave because of free streaming along the field lines. On the other hand, ions are essentially cold and respond to the cE_θ/B_0 drift which, in turn, generates local charge separation and therefore strong radial electric field. In fact, the ion $c\vec{E} \times \vec{B}$ flows form two-dimensional vortex or convective cell, as studied earlier in detail.⁷ The number of convective cells is much more than that of unstable drift modes; and the nonlinear interaction among convective cells can easily lead the plasma into a strong-turbulence state because of very effective $c\vec{E} \times \vec{B}/B^2$ mixing.

As the drift waves ($n=1$) grow in accordance with the linear theory, it is observed that the convective cells grow at about twice the growth rate of the drift waves when the drift waves reach at finite amplitude indicating the nonlinear excitation mechanism of the convective cells.⁸ It should be emphasized that the convective cells ($k_\parallel=0$) alone are stable in a collisionless plasma, as proved by the two-dimensional simulations.⁹

Figure 3 shows the formation of convective cells and ion diffusion due to nonlinear interactions among cells. Plotted are the guiding center

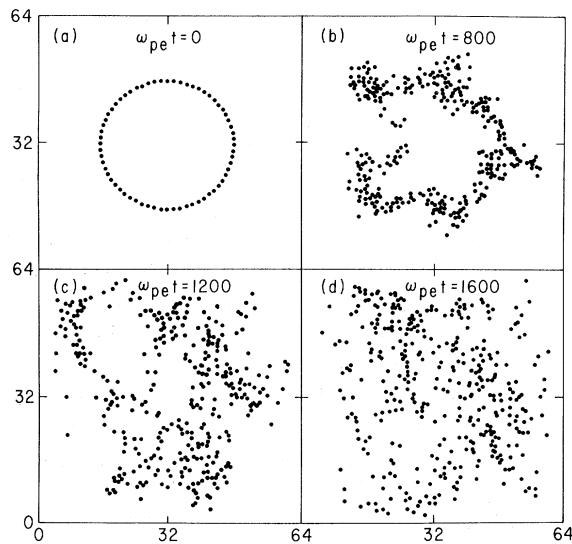


FIG. 3. Plot of the guiding center orbits of test ions initially sampled to form a ring at some fixed Z . Note the development of closed patterns of the flow due to radial field (c) and coalescence into larger cells (d).

orbits of the test ions initially sampled to form a ring at $r/a=0.5$. At early times, the test ions respond to cE/B_0 drift and one sees that several m modes are excited. As the instability develops, ion motion becomes highly nonlinear and tends to form vortex structure as a result of the generated radial electric field as clearly seen in the figure. Small cells eventually coalesce into larger cells and the ions diffuse across the entire plasma column in accordance with the development of large $m=1$ mode at $\omega=0$ as shown in Fig. 2(c).

In order to confirm the importance of convective cells on plasma diffusion, we carried out another simulation with the same parameters except that the two-dimensional modes ($k_z=0$) are artificially suppressed in the code. Figure 4 indicates the electron diffusion with and without $k_z=0$ modes. At early state ($\omega_{pe}t=1000$), diffusion is mainly due to drift instability, and little difference is observed for both cases. At the later stage, however, diffusion without convective modes is substantially smaller than the other case, and diffusion stops completely as the drift instability saturates and the finite density gradient is maintained. For the other case, convective cells eventually flatten the density profile completely even when the drift instability has been quenched by nonlinear effects. This observation has an important significance in the understanding of anomalous diffusion in laboratory experiments. While the convective cells are marginally

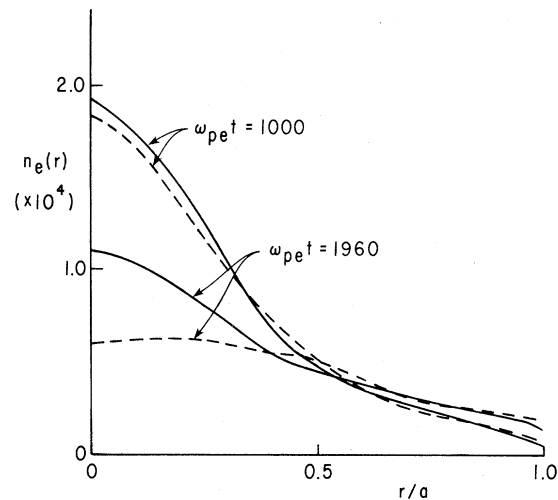


FIG. 4. Comparison of electron density diffusion with and without convective cells ($k_{||}=0$). Note that at $\omega_{pe}t=1960$, convective cells have larger amplitudes than the drift waves when the convective cells are not deleted.

stable,⁸ drift or trapped-particle instabilities can excite the convective cells, which then cause large diffusion even when the drift instabilities saturate nonlinearly. In a steady-state experiment, where the energy input such as that from ohmic heating and particle recycling balances with the anomalous diffusion, it is likely that the diffusion due to drift instabilities is small and the steady state is established by balancing the energy source with the convective diffusion.

The observed overall diffusion coefficient is about $1.6 \times 10^{-2} \rho_i^2 \omega_{pe}^{-1}$, which is close to the convective diffusion⁷ $D_{\perp} = 2.0 \times 10^{-2} \rho_i^2 \omega_{pe}^{-1}$ when the saturated amplitude of the convective cells are used.¹⁰ The saturation amplitude is more than 10^2 times larger than the initial noise amplitude of the convective cells. The usual estimate of diffusion $D_{\perp} = \gamma/k_{\perp}^2 \approx 10^{-2}$ is also close to the observation.

It is interesting to compare our results with recent laboratory experiments in toroidal devices. Recent results of Hamberger *et al.*³ indicate that for very strong shear ($L_s/L_n=7$), the power spectrum shows a well-defined peak near the drift frequency. As the shear is reduced, a new peak appears near $\omega \approx 0$; and further reduction of shear results in a turbulent spectrum with no well-defined peaks.² The two-peak spectrum shown in Fig. 2 resembles that of Hamberger *et al.* Similar result is reported for the Culham Levitron experiment of Alcock *et al.*⁵

While our power spectrum is not as broad as those in the toroidal experiments with weak shear, the spectrum in the simulation is measured in a transient state from initial linear phase to the final turbulent state while the laboratory experiments measure fully developed steady-state turbulence driven externally. Furthermore, the spectrum in the laboratory experiments is averaged over different k_{\parallel} modes and the plasma radius. The simulation spectrum will be monotonic if such averaging is carried out.

We have simulated the same example, keeping 11 modes in z ($n=0, \pm 1, \dots, \pm 5$), and found the results essentially the same. We have also included a magnetic shear in the simulations and found the convective cells to persist for $L_s/L_n \lesssim 25$. The details will be reported later.⁸

We acknowledge useful discussions with Dr. W. Lee, Dr. V. Arunasalum, and Dr. M. Okabayashi.

*Work supported by the U. S. Energy Research and Development Administration under Contract No. E(11-1)-3073.

¹C. Z. Cheng and H. Okuda, to be published, and

Princeton Plasma Physics Laboratory Report No. PPPL-1204, 1976 (unpublished).

²E. Mazzucato, Phys. Rev. Lett. **36**, 792 (1976).

³S. M. Hamberger, L. E. Sharp, J. B. Lister, and S. Mrowka, Phys. Rev. Lett. **37**, 1345 (1976).

⁴M. Okabayashi and V. Arunasalum, Princeton Plasma Physics Laboratory Report No. PPPL-1310, 1976 (unpublished).

⁵M. W. Alcock, D. E. T. F. Ashby, J. G. Gordey, T. Edlington, W. H. W. Fletcher, E. M. James, J. Malmberg, A. C. Riviere, D. F. H. Start, and D. R. Sweetman, in Proceedings of the Sixth International Conference on Plasma Physics and Controlled Fusion, Berchtesgaden, West Germany, 6-13 October, 1976 (International Atomic Energy Agency, Vienna, to be published).

⁶W. W. Lee and H. Okuda, Phys. Rev. Lett. **12**, 870 (1976).

⁷H. Okuda and J. M. Dawson, Phys. Fluids **16**, 408 (1973).

⁸H. Okuda and C. Z. Cheng, Princeton Plasma Physics Laboratory Report No. PPPL-1328 (to be published).

⁹J. Canosa, J. Krommes, C. Oberman, H. Okuda, K. Tsang, J. M. Dawson, and T. Kamimura, in *Proceedings of the Fifth International Conference on Plasma Physics and Controlled Nuclear Fusion Research, Tokyo, Japan, 1974* (International Atomic Energy Agency, Vienna, Austria, 1975), p. 177.

¹⁰J. B. Drake, J. R. Greenwood, G. A. Navratil, and R. S. Post, Phys. Fluids **20**, 148 (1977).

Chain-Pairing Effects in One-Dimensional Conjugated Polymers and Semiconductors

G. P. Agrawal, C. Cojan, and C. Flytzanis

Laboratoire d'Optique Quantique, Ecole Polytechnique, 91128 Palaiseau, France*

(Received 20 December 1976)

We explain the absorption line and resonant Raman lines splittings together with the selection rules at low temperatures in polydiacetylene polymer crystals in terms of a chain-pairing mechanism arising from side-group interactions between the conjugated carbon chains. The symmetry of the pairing configuration has drastic effects on the one- and two-photon absorption spectra.

The availability of large defect-free crystals on the solid-state polymerization¹ of diacetylene monomers $R-C\equiv C-C\equiv C-R$, R being a radical, has triggered a growing interest in this new class of materials. Large separation among the chains and bond alternation along the conjugated carbon chains² confer to these materials an insulator-type behavior across the chains but a semiconducting one along the chain direction. This is reflected³ in an intense and relatively narrow absorption peak around 2 eV at room temperature arising from π -electron transitions.

It has recently been established^{4,5} that at lower temperatures, below 160°K for the polydiacety-

lent-*bis* toluene sulphonate (PTS diacetylene, $R=CH_2-O-SO_2-\Phi-CH_3$), the peak splits into two narrow and equally intense lines, the separation between them increasing with decreasing temperature and reaching a value $\approx 500 \text{ cm}^{-1}$ at 4°K for the PTS-diacetylene. Such a remarkable behavior is also observed⁶ in the resonant Raman scattering (RRS) spectra. Furthermore, around the same temperature the system probably undergoes⁷ a phase transition doubling the unit-cell dimensions along the crystallographic a axis (the b axis is the chain direction). It has been verified that these splittings are not due to the appearance of two different chains per unit cell and